

Calculation of Adjoint Flux Distribution Using Iterated Fission Probability Method in the iMC Monte Carlo Code

Taesuk Oh^a, Inyup Kim^a, and Yonghee Kim^{a*}

^a Nuclear and Quantum Engineering, Korea Advanced Institute of Science and Technology (KAIST),
291 Daehak-ro, Yuseong-gu, Daejeon 34141, Republic of Korea

*Corresponding author: yongheekim@kaist.ac.kr

***Keywords** : Monte Carlo (MC), Iterated Fission Probability (IFP), Adjoint Flux, iMC Code

1. Introduction

With recent significant advancements in computing resources, the Monte Carlo (MC) approach for practical reactor analysis, particularly in cross-section generation for lattice calculations, has garnered increased attention [1]. Fundamental aspects of a reactor system encompass the multiplication factor, power distribution, and adjoint-weighted effective kinetic parameters. While the mathematical foundations for the former two quantities were laid down during the initial introduction of the MC method, the determination of effective kinetic parameters remained ambiguous until the emergence of the Iterated Fission Probability (IFP) method in the late 2000s [2-3].

The determination of effective kinetic parameters in MC simulations requires the implementation of an adjoint flux-weighted tally. While one might consider pre-calculating an adjoint flux distribution using a 'backward' approach, the inherent ambiguity in the inversion of scattering laws, requiring particles to scatter opposite to the normal energy transfer, makes backward continuous-energy MC calculations challenging [4].

In contrast, the IFP method addresses adjoint information by tracking the evolution of source neutrons throughout cycles. This approach eliminates the need for the direct calculation of adjoint flux to assess effective kinetic parameters and has proven successful in various MC codes, including the iMC code developed at the Korea Advanced Institute of Science and Technology (KAIST) [5-6].

Beyond the calculation of effective kinetic parameters, involving integration over the entire phase-space, there is potential for a phase-space-wise integration to assess the distribution of adjoint information [7-8]. This paper presents IFP-based adjoint flux calculation results for various benchmarks using the iMC code, with comparisons made against deterministic results for validation purposes.

2. Iterated Fission Probability (IFP) Method

The adjoint flux is a measure of the significance of particles generated at a specific phase-space point $\theta(\vec{r}_0, \vec{\Omega}_0, E_0)$ in contributing to fission reactions. In the context of a steady-state reactor scenario, where the fission source distribution ultimately reaches

convergence, the mathematical representation of the extent of fission reactions originating from a source neutron at a given phase-space also converges. Expanding on this interpretation, the Iterated Fission Probability (IFP) is defined as the asymptotic count of fission neutrons arising from a neutron at phase-space θ , and this definition is mathematically identical to the adjoint flux [2].

In practice, a certain number of cycles, which is referred to as a latent cycle (L), must pass to approach the asymptotic power. Hence, by tracking the fission-born neutrons throughout the cycles, which are referred to as progenies, the IFP quantity for the phase-space of interest can be deduced. Note that the original source of progenies that have been banked L cycles before is referred to as progenitor.

The acquired IFP information throughout the cycle is then used for calculating the effective kinetic parameters. Note that the integration is performed over the whole phase-space, i.e., point reactor model.

The effective delayed neutron fraction for the k^{th} group ($\beta_{d,k}$) is obtained as:

$$\beta_{d,k} = \frac{\left\langle \varphi^\dagger(\vec{r}, E, \vec{\Omega}), \frac{\chi_{d,k}(E)}{4\pi} F_{d,k} \varphi(\vec{r}, E, \vec{\Omega}) \right\rangle}{\left\langle \varphi^\dagger(\vec{r}, E, \vec{\Omega}), \frac{\chi(E)}{4\pi} F \varphi(\vec{r}, E, \vec{\Omega}) \right\rangle}, \quad (1)$$

where bracket denotes phase-space integration, φ^\dagger is the adjoint flux, $\chi(E)$ denotes the fission spectrum, and notations $F\varphi$ and $F_{d,k}\varphi$ are defined as below:

$$F\varphi(\vec{r}, E, \vec{\Omega}) = \int d\vec{\Omega}' \int dE' \nu \sigma_f(\vec{r}, E') \varphi(\vec{r}, E', \vec{\Omega}'), \quad (2)$$

$$F_{d,k}\varphi(\vec{r}, E, \vec{\Omega}) = \int d\vec{\Omega}' \int dE' \nu_{d,k} \sigma_f(\vec{r}, E') \varphi(\vec{r}, E', \vec{\Omega}'). \quad (3)$$

The effective generation time can be calculated as following:

$$\Lambda = \frac{\left\langle \varphi^\dagger(\vec{r}, E, \vec{\Omega}), \frac{1}{v(E)} \varphi(\vec{r}, E, \vec{\Omega}) \right\rangle}{\left\langle \varphi^\dagger(\vec{r}, E, \vec{\Omega}), \frac{1}{k_0} \frac{\chi(E)}{4\pi} F \varphi(\vec{r}, E, \vec{\Omega}) \right\rangle} \quad (4)$$

where k_0 is the multiplication factor for the steady-state, and $v(E)$ is the speed of the neutron of interest.

Similar to the methodology employed in evaluating effective kinetic parameters, the integration of adjoint flux weighting can be executed within a designated phase-space range of interest. This enables the preservation of representative position and energy details, essentially capturing the phase-space dependency.

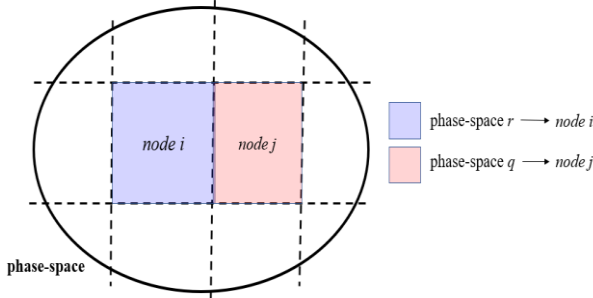


Fig 1. Schematic for tallying adjoint flux distribution.

Consequently, one can consider tallying the adjoint-weighted variable within a mesh-based framework. To approximate the mesh-based representation of adjoint flux information, illustrated in Fig. 1, the following approach is applied:

$$\varphi_i^\dagger(\vec{r}, E, \vec{\Omega}) \approx \frac{\langle \varphi^\dagger(\vec{r}, E, \vec{\Omega}), \varphi(\vec{r}, E, \vec{\Omega}) \rangle_r}{\langle 1, \varphi(\vec{r}, E, \vec{\Omega}) \rangle_r}, \quad (5)$$

where subscript r for the integration indicates phase-space range of interest and its corresponding representative phase-space values for mesh-based description, e.g., node i , are denoted as $(\vec{r}_i, E_i, \vec{\Omega}_i)$.

The denominator of Eq. (5) can be tallied using the track length estimator for the flux

$$\langle 1, \varphi(\vec{r}, E, \vec{\Omega}) \rangle_r = \frac{1}{V_r} \sum_T w l \delta_{r,q}, \quad (6)$$

where the summation is performed over all particle tracks T residing within the phase-space range of interest denoted as r . Notations w and l are the weight and track length of the particle, and V_r is the volume corresponding to the phase-space range of interest. The current phase-space information of the particle track is represented as q and $\delta_{r,q}$ is the Kronecker delta function being unity if and only if when $q \in r$.

To tally the numerator of Eq. (5), which is the adjoint flux-weighted forward flux, the following approach is taken:

$$\langle \varphi^\dagger(\vec{r}, E, \vec{\Omega}), \varphi(\vec{r}, E, \vec{\Omega}) \rangle_r = C \frac{1}{V_r} \sum_p w_0 l_s \delta_{rs} \sum_{T \in p} v \Sigma_f l, \quad (7)$$

where C is an arbitrary constant depending on the characteristics of the detector response function, and subscript p represents the source of progeny, i.e.,

progenitor, which is the banked neutron source during transport process. The weight w_0 corresponds to the initial weight of the particle born from the progenitor, and l_s is the track length of such a particle that results in a fission reaction for its asymptotic population, where the subscript s represents the phase-space information of the particle. Note that the fission reaction term in Eq. (7), which embodies the adjoint flux information, is evaluated for particle tracks T which originate from the progenitor after passing the latent cycles (L), i.e., asymptotic population.

3. Numerical Results

As aforementioned, the iMC code incorporates the IFP method for the assessment of effective kinetic parameters and adjoint flux distribution. To validate the effective kinetic parameter tallying, a comparison has been conducted with the validated Serpent 2 MC code for the VERA 1A and 1B benchmarks [9]. Both iMC and Serpent 2 assumed 15 latent cycles, comprising 100 inactive cycles followed by 500 active cycles, with 400,000 histories per cycle with ENDF/B-VII.1 library. Tables 1 and 2 enumerate the calculated results respectively, where reasonable agreement between the codes can be observed.

Table 1. VERA 1A benchmark result

Values	Serpent2	iMC
k_{eff} [-]	1.18718 (3.9)	1.18711 (6.5)
β_{eff} [pcm]	687.3 (2.6)	683.7 (1.9)
β_1 [pcm]	21.6 (0.5)	21.0 (0.3)
β_2 [pcm]	117.1 (1.0)	117.9 (0.8)
β_3 [pcm]	114.0 (1.0)	114.4 (0.7)
β_4 [pcm]	264.3 (1.6)	263.0 (1.2)
β_5 [pcm]	120.9 (1.1)	117.9 (0.8)
β_6 [pcm]	49.5 (0.7)	49.5 (0.5)
Λ [10^{-9} s]	17916.5 (6.3)	17911.1 (4.5)

*Uncertainty of 1σ given within the bracket.

Table 2. VERA 1B benchmark result

Values	Serpent2	iMC
k_{eff} [-]	1.18222 (4.1)	1.18222 (6.5)
β_{eff} [pcm]	686.3 (2.6)	686.7 (1.8)
β_1 [pcm]	21.5 (0.4)	21.6 (0.3)
β_2 [pcm]	114.3 (1.0)	117.5 (0.8)
β_3 [pcm]	113.4 (1.0)	112.9 (0.8)
β_4 [pcm]	265.8 (1.6)	264.1 (1.1)
β_5 [pcm]	121.5 (1.1)	120.0 (0.8)
β_6 [pcm]	49.8 (0.7)	50.6 (0.5)
Λ [10^{-9} s]	18072.9 (6.5)	18078.1 (4.8)

*Uncertainty of 1σ given within the bracket.

To assess the applicability of Eq. (5) for estimating adjoint flux distribution, a one-group one-dimensional slab reactor having a length of 20 cm with the following cross-sections have been considered:

Table 3. One-group cross-sections for the slab reactor.

Cross-sections	Values
Σ_t	1.0 cm ⁻¹
Σ_a	0.3 cm ⁻¹
Σ_f	0.2 cm ⁻¹
Σ_s	0.7 cm ⁻¹
ν	1.5 [-]

The deterministic adjoint solution was obtained through an in-house code based on the discrete ordinate method ($S_{N=20}$) with Gauss-Legendre quadrature set and a spatial discretization of 0.05 cm

$$-\vec{\Omega} \cdot \nabla \varphi^\dagger(\vec{r}, \vec{\Omega})|_{\vec{\Omega}_n} + \sigma(\vec{r})\varphi^\dagger(\vec{r}, \vec{\Omega}_n) = q^\dagger(\vec{r}, \vec{\Omega}_n), \quad (8)$$

where all the notations are that of the convention [10]. Both vacuum and reflective boundary conditions are expressed as:

$$\varphi^\dagger(\vec{r}_s, \vec{\Omega}_n) = 0 \quad (\hat{n}_s \cdot \vec{\Omega}_n > 0), \quad (9a)$$

$$\varphi^\dagger(\vec{r}_s, \vec{\Omega}_n) = \varphi^\dagger(\vec{r}_s, \vec{\Omega}_m) \quad (\hat{n}_s \cdot \vec{\Omega}_n > 0), \quad (9b)$$

respectively, with ordinates $\vec{\Omega}_n$ and $\vec{\Omega}_m$ ($n \neq m$) satisfy

$$\hat{n}_s \cdot \vec{\Omega}_n = -\hat{n}_s \cdot \vec{\Omega}_m, \quad (10)$$

$$\hat{n}_s \cdot (\vec{\Omega}_n \times \vec{\Omega}_m) = 0.$$

In the iMC calculation, a spatial discretization of 0.5 cm was utilized for tallying Eq. (5). Figure 2 illustrates a comparison of the results, considering various latent cycle numbers. It is evident that an insufficient number of latent cycles introduces noticeable bias, with a recommended minimum of 14 latent cycles. It is important to note that the uncertainty range of the Iterated Fission Probability (IFP)-based adjoint flux is marginal, a detail not visually discernible from the markers and therefore omitted throughout this work.

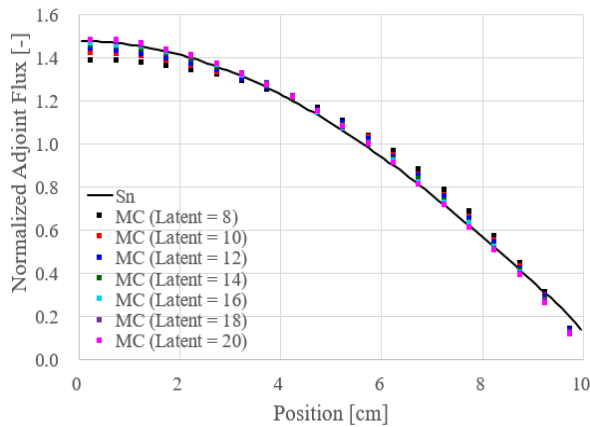


Fig 2. Adjoint flux distribution for slab reactor with various number of latent cycles.

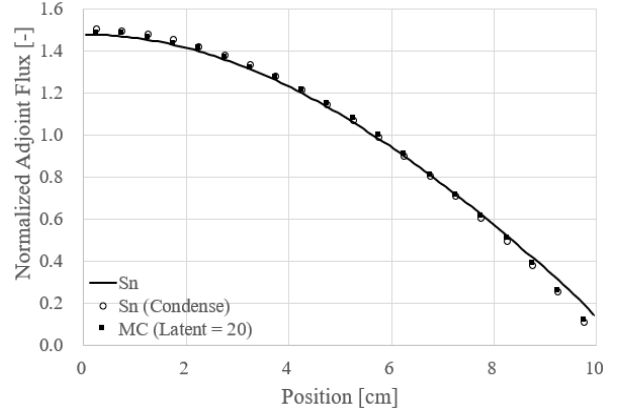


Fig 3. Condensed adjoint flux distribution

Figure 3 presents the condensed results from deterministic angular flux, employing the same node size as the MC simulation in accordance with Eq. (5). Both the Monte Carlo and condensed deterministic solutions exhibit strong agreement, although they deviate from the fine-mesh-wise S_{20} result.

Analogous to the spatial distribution, an energy-dependent adjoint flux (or spectrum) can be derived, encompassing both multi-group (MG) and continuous-energy (CE) problems for validation purposes. In the MG scenario, a pin-cell from the C5G7 benchmark is considered, where a comparison is made with respect to the deterministic solution based on the Method of Characteristics (MOC) as shown in Fig. 4 [11]. Note that the iMC solution postulated latent cycle number of 15.

In the context of the continuous-energy (CE) problem, the previously mentioned VERA 1A configuration has been considered. The adjoint spectrum was computed using the HELIOS 47 group structure, and a comparison was conducted with the physical adjoint obtained from the MOC solution [11]. The results are illustrated in Fig. 5, where variation in the latent cycle number is considered. It can be seen that a reasonable agreement is met between the solutions, even with a latent cycle number of 10. This suggests that the adjoint spectrum may exhibit relatively less sensitivity to the latent cycle number compared to the spatial adjoint flux distribution.

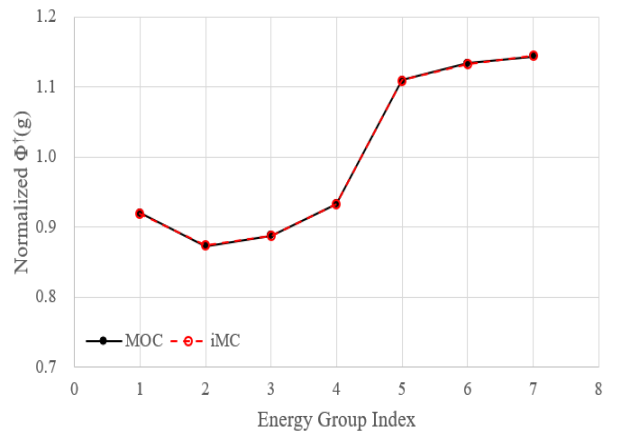


Fig 4. Adjoint spectrum for C5G7 pin-cell problem.

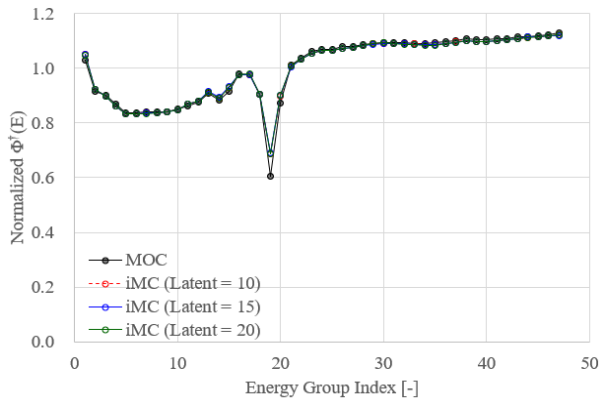


Fig 5. Adjoint spectrum for VERA 1A problem.

4. Conclusions

In this study, the concept of iterated fission probability (IFP) and its application for estimating both adjoint flux weighted effective kinetic parameters and distribution of adjoint flux have been investigated using the iMC Monte Carlo code. The IFP method involves tracking the source of fission-born neutrons and their progenies over a sufficient number of latent cycles to enable the tallying of the integral form of the effective kinetic parameters. In the assessment of the adjoint flux distribution, a mesh-based representation is envisaged, wherein adjoint weighted flux values are recorded for each node. Subsequently, by dividing with the mesh-based flux distribution, the adjoint flux distribution can be determined.

To validate the computed effective kinetic parameters, the VERA 1A and 1B benchmarks were employed, and the results were compared with those obtained from Serpent 2. Spatial tallying of the adjoint flux distribution was conducted for a one-group one-dimensional slab reactor, while considering both multi-group and continuous-energy pin cell problems for the adjoint spectrum. The tallied adjoint flux distribution was subsequently compared with deterministic transport solutions. The obtained results consistently demonstrated a reasonable agreement, affirming the suitability of the IFP-based solution computed using the iMC code. As part of future research endeavours, emphasis will be placed on algorithmic enhancements aimed at optimizing computing efficiency for IFP-based evaluations.

ACKNOWLEDGEMENTS

This work was supported by the National Research Foundation of Korea Grant funded by the Korean government NRF-2021M2D2A2076383

REFERENCES

[1] J. Leppänen, M. Pusa, T. Viitanen, V. Valtavirta, and T. Kaltiaisenaho, "The Serpent Monte Carlo code: Status, development and applications in 2013," *Ann. Nucl. Energy*, vol. 82, pp. 142–150, 2015.

[2] Y. Nauchi and T. Kameyama, "Development of Calculation Technique for Iterated Fission Probability and Reactor Kinetic Parameters Using Continuous-Energy Monte Carlo Method", *Journal of Nuclear Science and Technology*, Vol. 47, No. 11, p.977-990, 2010.

[3] Brian C. Kiedrowski, Forrest B. Brown and Paul P. H. Wilson, "Adjoint-Weighted Tallies for k-Eigenvalue Calculations with Continuous-Energy Monte Carlo", *Nucl. Sci. Eng.*, 168, 226-241, 2011.

[4] J. E. Hoogenboom, "Methodology of continuous-energy adjoint Monte Carlo for neutron, photon, and coupled neutron-photon transport", *Nucl. Sci. Eng.*, 143[2], 99–120 (2003).

[5] Inyup Kim, Tae-suk Oh, and Yonghee Kim, "Modeling of Effective Delayed Neutron Fraction in the Monte Carlo iMC code for Flowing Fuel Reactors", *Transactions for the Korean Nuclear Society Spring Meeting, Jeju, Korea, May 19-20 (2022)*.

[6] Tae-suk Oh, Inyup Kim, and Yonghee Kim, "Implementation of Iterated Fission Probability Method for Calculating Effective Kinetic Parameters and Adjoint Flux Distribution in the iMC Monte Carlo Code", *Transactions for the Korean Nuclear Society Spring Meeting, Jeju, Korea, May 18-19 (2023)*.

[7] Nicholas Terranova et al., "Adjoint neutron flux calculations with TRIPOLI-4: Verification and comparison to deterministic codes", *Annals of Nuclear Energy* 114 (2018) 136-148.

[8] Francesco Tantillo and Simon Richards, "Adjoint neutron flux estimator implementation and verification in the continuous energy Monte Carlo code MONK", *Nuclear Engineering and Design* 356 (2020) 110368.

[9] Godfrey, Andrew T. "VERA core physics benchmark progression problem specifications." Consortium for Advanced Simulation of LWRs (2014).

[10] E. E. Lewis and W. F. Miller, Jr., "Computational Methods of Neutron Transport", John Wiley & Sons, New York, 1984.

[11] Kaijie Zhu, Chen Hao, and Yunlin Xu, "Advanced two-level CMFD acceleration method for the 3D whole-core high-fidelity neutron adjoint transport calculation", *Nuclear Engineering and Technology* 53 (2021) 30-43.